

# Mechanistic Interpretation for Xanthate Adsorption onto Galena through Electrochemical Impedance Spectrum Fitting by a Differential Evolution Algorithm

*E.D. Moreno-Medrano*<sup>1\*</sup>, *Valentín Osuna-Enciso*<sup>1</sup>, *N. Casillas*<sup>2</sup>, *M. A. Pedroza-Toscano*<sup>3</sup>,  
*A. Gutierrez-Becerra*<sup>1</sup>, *E.R. Larios-Durán*<sup>4</sup>

<sup>1</sup> Engineering and Basic Sciences Department, University of Guadalajara, CUTonalá, 48525, México; edgar.mmedrano@academicos.udg.mx, valenteos@hotmail.com, algubec@gmail.com

<sup>2</sup> Chemistry Department, University of Guadalajara, CUCEI. Gdl., 44430, México; ncasa@hotmail.com

<sup>3</sup> University Center UTEG, Gdl. 44430, México; mpedroza@uteg.edu.mx

<sup>4</sup> Chemical Engineering Department, University of Guadalajara, CUCEI. Gdl., 44430, México; eroxanita@gmail.com

\*E-mail: [edgar.mmedrano@academicos.udg.mx](mailto:edgar.mmedrano@academicos.udg.mx)

*Received:* 15 August 2019 / *Accepted:* 18 October 2019 / *Published:* 30 November 2019

---

This work is focused on understanding the interaction of native galena minerals and xanthate as well as their influence on the process of mineral separation by flotation and leaching techniques. To obtain basic and fundamental information about this interaction, a quantitative analysis of an electrochemical impedance study based on a mechanistic approach and the obtaining of its impedance transfer function is presented. The impedance transfer function was obtained from a three-reversible-stage mechanism, which included 19 parameters, all of which were satisfactorily obtained by fitting the impedance transfer function to previously reported experimental impedance spectra of the galena/xanthate interface in a wide polarization potential range of -0.2 to 0.5 V vs. SCE. The fitting procedure consisted of the application of a differential evolution (DE) algorithm. The description of this algorithm, its application and its advantages in the electrochemical impedance field are presented. Furthermore, a detailed discussion about the quantitative values obtained and its interpretation for galena/xanthate interactions is presented.

---

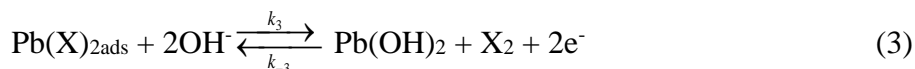
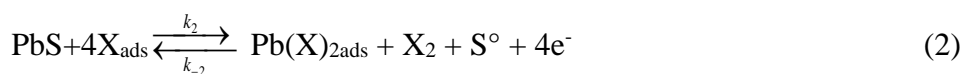
**Keywords:** galena, xanthate, impedance, adsorption mechanics, differential evolution algorithm.

## 1. INTRODUCTION

Obtaining fundamental information on the electrochemical interactions of galena/xanthate (PbS/X) could allow better control over the flotation processes of sulfurous minerals, which are

processes extremely important for the mining industry. In this sense, we are interested in studying the adsorption kinetics of sodium isopropyl xanthate during anodic oxidation of galena. For this, electrochemical impedance spectroscopy (EIS) and its interpretation from a mechanistic approach are used. The interpretation of impedance spectra under this approach is an unexplored or little explored strategy; however, it allows a detailed physical and kinetic description of the systems. This approach has been used to study systems including methanol oxidation on platinum [1], electrodisolution of gold [2], continuous glucose monitoring [3], corrosion mechanism of magnesium [4] and others [5,6]. However, there are no similar investigations for the PbS/X system; therefore, the aim of this work is to obtain the experimental impedance spectra and then compute and adequately fit the experimental impedance spectra for the PbS/X system via a mechanistic approach to obtain kinetic and physical-chemical information of the interface.

In accordance with other investigations [7-15], the following reaction mechanism for the oxidation of galena in the presence of xanthate has been established:



where the subscript ads stand for adsorbed intermediate.

This mechanism includes three reversible reactions: reaction 1 corresponds to the adsorption of xanthate  $(X)_{\text{ads}}$  on the galena surface; reaction 2 involves the formation of dixanthogen  $(X_2)$ , lead xanthate  $(\text{Pb}(X)_2)$  and elemental sulfur; and reaction 3 involves the formation of lead hydroxide  $(\text{Pb}(OH)_2)$ .

Fitting impedance spectra of experimental reaction mechanisms is a complicated task because this type of model considers the tuning of several parameters that are contained into a real multidimensional numeric space. Accordingly, the utilization of optimization tools is a natural step to be considered for solving the aforementioned fitting. From that perspective, two approaches [16] could be contemplated: 1) exact methods, which rely on certain information about the mathematical function being optimized (such as the first or second derivative, etc.); and 2) approximated techniques, which are based on a certain degree on stochastic searches that produce near-optimal solutions in more flexible ways than the first mentioned approach. In the second category, evolutionary algorithms (EA) [17] are the most utilized method to solve optimization problems in areas such as manufacturing industries [18], energy production [19], and chemical engineering [20]. In EA, a population of candidate solutions is improved by means of evolutionary mathematical operators to find the best one that solves a given optimization problem. Differential evolution (DE) is a known EA that was proposed by Storn and Price as a global optimizer [21] and shows several advantages against those of the other EAs, namely: 1) robustness, 2) few parameters to tune, and 3) good convergence properties. Accordingly, in this article, the differential evolution algorithm is used to solve the problem of impedance spectrum fitting for the PbS/X system. The study of PbS/X systems by impedance measurements has been previously reported

[14]; however, a detailed explanation from a kinetic and mechanistic point of view is lacking even when the information that could be obtained from it is highly desired.

In this way, the spectra measured previously [14] are revisited, and its interpretation is carried out by a mechanistic approach. A detailed analysis of each kinetic and thermodynamic parameter obtained from the fitting using DE and its behavior as a function of the polarization potential range studied is presented in this paper.

## 2. EXPERIMENTAL PROCEDURE

### 2.1 Obtaining the transfer function

As the first stage, from reactions (1), (2) and (3), a mathematical model for the oxidation of galena in the presence of xanthate is proposed. This model includes transfer functions for total and faradaic impedance, which were rearranged according to the reaction or reactions that take place at the interface (depending on polarization potential). Then, the transfer functions were programmed and simulated using MATLAB® to generate the theoretical impedance spectra predicted by the proposed mechanism. These spectra were fitted to the experimental impedance spectra for the PbS/X system obtained by Moreno-Medrano et al. [14]. The working electrode used was native galena with a potential range (E) between -0.5 V and 0.2 V (vs SCE) in the presence of 0.1 M xanthate at pH 8 and KCl as the supporting electrolyte at 25 °C. For the fitting procedure, the DE algorithm was consecutively applied until a good agreement between the experimental and theoretical data was reached, which was generally obtained after 30 iterations. The number of iterations carried out for each spectrum was optimized via differential evolution and is detailed in the next section.

### 2.2 Optimization via differential evolution

In this work, we consider the fitting between the theoretical impedance spectra and the experimental spectra as an optimization problem, in this case represented as the added squared difference among them, which can therefore be minimized via DE as an optimization tool:

$$\min f(x) = d(Z_s^i, Z_E^i) = \sum_{i=1}^N (Z_s^i - Z_E^i)^2 \quad (4)$$

where  $Z_s$  is the simulated spectra,  $Z_E$  is the experimental spectra, which is a vector of constant values,  $N$  is the number of points in the spectra, and  $x$  is the candidate solution (also called the decision variable), which is composed of the tuning parameters of  $Z_s$ :

$$x = \{\beta_1, \beta_2, k_{10}, k_{-10}, k_{20}, k_{-20}, k_{30}, k_{-30}, a, b, c, d, e, f, R_s, C_{dl}, n, Pb(OH)_2\} \quad (5)$$

Here,  $\beta_1$  and  $\beta_2$  are mol of adsorbed species onto the surface electrode, mol/cm<sup>2</sup>, and  $k_{i0}$ ,  $a$ ,  $b$ ,  $c$ ,  $d$ ,  $e$  and  $f$  are constants associated with the electrochemical rate constants in the following form:

$$k_1 = k_{10}e^{aE}, k_{-1} = k_{10}e^{-bE}, k_2 = k_{20}e^{cE}, k_{-2} = k_{20}e^{-dE}, k_3 = k_{30}e^{eE}, k_{-3} = k_{30}e^{-fE}$$

where  $E$  is the polarization potential (V),

$R_s$  is the solution resistance ( $\Omega$ ),

$C_{dl}$  is double-layer capacitance (F),

$n$  is the exponential parameter included at the constant-phase element (CPE),

$C_{dl}(j\omega)^n$ , where  $j$  is the imaginary number and where  $\omega$  is the frequency (rad/s) [22].

To efficiently explore the solution space ( $\mathbf{x} \in \mathbb{R}^D$ , and  $D=18$ , which is the dimension of the problem), in this article, a canonical version of DE is utilized [21]. This algorithm has four basic steps: 1) initialization, 2) mutation, 3) recombination, and 4) selection; in practice, steps 2-4 are repeated until a given condition is met, usually until a number of iterations is reached. In the first step, a population  $\mathbf{x}$  composed of vectors of candidate solutions  $\mathbf{x}_i$  is initialized by means of

$$\mathbf{x}_i = \mathbf{x}^l + \mathbf{rand}^*(\mathbf{x}^u - \mathbf{x}^l) \tag{6}$$

where  $\mathbf{rand}$  is a vector of uniform random numbers,  $i=1\dots,N_P$ ,  $N_P$  is the population size, and  $\mathbf{x}^u$  and  $\mathbf{x}^l$  are the upper and lower limits, respectively, of the search space in where the solution is contained:

$$\begin{aligned} \mathbf{x}^u &= \{1^{-6}, 1^{-6}, 2^{-1}, 2^{-1}, 2^{-1}, 4500, 1, 2^{-1}, 200, 200, 200, 200, 200, 200, 60, 2^{-1}, 1, 2^{-1}\} \\ \mathbf{x}^l &= \{0, 0, 0, 0, 0, 0, 0, -1000, -5000, -1000, -1000, -1000, -1000, -1000, -100, 0, 0, 0\} \end{aligned} \tag{7}$$

The upper and lower limits shown in (7) were established based on previous work [14].

In the DE version used in this work, the mutation strategy considers the best individual,  $\mathbf{x}_{best}$ , found so far, and the weighted difference between two randomly selected individuals of the population,  $\mathbf{x}_{r1}$ ,  $\mathbf{x}_{r2}$ ; to compound the mutant vector  $\mathbf{v}_i$ , which is also called the donor vector:

$$\mathbf{v}_i = \mathbf{x}_{best} + H(\mathbf{x}_{r1} - \mathbf{x}_{r2}) \tag{8}$$

Consider that 1)  $r_1$ ,  $r_2$  are both integer random numbers used to select two random parents from the population that comply with  $r_1 \neq r_2 \neq i$  and 2)  $H$  is a scaling parameter for the parents difference. For the third step, the binomial (also called uniform) crossover, which employs the original candidate solution  $\mathbf{x}_i$  together with the donor vector  $\mathbf{v}_i$ , is used to compound the offspring or trial vector  $u_{i,j}$ :

$$u_{i,j} = \begin{cases} v_{i,j} & \text{if } j = j_{rand} \mid rand \leq Cr \\ x_{i,j} & \text{otherwise} \end{cases} \tag{9}$$

where  $Cr$  is a crossover parameter,  $j_{rand}$  is a uniform integer number in  $\{1\dots,D\}$ , and  $rand$  is a uniform number in  $[0,1]$ . Finally, in the last phase, the trial vector competes against the candidate vector:

$$\mathbf{x}_i^{k+1} = \begin{cases} \mathbf{u}_i^k & \text{if } f(\mathbf{u}_i^k) \leq f(\mathbf{x}_i^k) \\ \mathbf{x}_i^k & \text{otherwise} \end{cases} \quad (10)$$

in consideration of  $k=1, \dots, \Omega$  where  $k$  and  $\Omega$  the actual iteration and the maximum iteration number, respectively.

### 3. RESULTS AND DISCUSSION

#### 3.1 Obtaining the transfer function

Based on reactions (1), (2) and (3), we obtained the transfer functions for faradaic and total impedance by applying a mass and current balance [23]. When the polarization potential is sufficiently anodic ( $E > 0.1$  V vs. SCE), reactions (1), (2) and (3) take place at the electrode interface, and the corresponding transfer functions are determined according to the following assumptions:

If the presence of two adsorbed intermediates that recover the electrode in a fractional proportion, with concentrations

$$\theta_1 = X_{ads}, \theta_2 = Pb(X)_{2ads}$$

$$[X_{ads}] = \beta_1 \theta_1 [Pb(X)_{2ads}]$$

where  $\beta_1$  represents the excess surface concentration for each intermediate given in mol/cm<sup>2</sup>; then, from a mass balance for both adsorbed intermediates,

$$\frac{d[X_{ads}]}{dt} = \beta_1 \frac{d\theta_1}{dt}, \quad \frac{d[Pb(X)_{2ads}]}{dt} = \beta_2 \frac{d\theta_2}{dt}$$

the fractional cover of the surface for at the steady state,  $s$ , ( $\frac{d\theta_n}{dt} = 0$ ) will be given by:

$$\theta_{1s} = \frac{-k_2 \beta_2 \theta_{2s} - [X^-] k_1 (\theta_{2s} - 1)}{\beta_1 (4k_2 + k_{-1}) + [X^-] k_1} \quad (11)$$

$$\theta_{2s} = \frac{k_{-3} [Pb(OH)_2] + \frac{k_2 \beta_1 \theta_{1s}}{4}}{\beta_1 (k_3 + k_{-2})} \quad (12)$$

Now, if the system is perturbed with a sinusoidal potential  $\Delta E = |\Delta E| \exp(j\omega t)$ , then the fractional recovery of the surface will variate in an exponential given by  $\Delta \theta = |\Delta \theta| \exp(j\omega t)$  and then,

$$\beta_n \frac{d\theta_n}{dt} = \beta_n j \omega \Delta \theta_n = \frac{\partial}{\partial E} \left[ \beta_n \frac{d\theta_n}{dt} \right]_s + \int \frac{\partial}{\partial \theta_n} \left[ \beta_n \frac{d\theta_n}{dt} \right]_s \Delta \theta_n$$

With this equation and from a mass balance for each adsorbed intermediate, their transfer functions are obtained as:

$$\frac{\Delta\theta_1}{\Delta E} = \frac{ak_1(1-\theta_{1s}-\theta_{2s})[X^-]-\beta_1\theta_{1s}(-bk_1+4ck_2)+dk_{-2}\beta_2\theta_{2s}}{(\tau_1j\omega+1)\{k_1[X^-]+\beta_1(k_{-1}+4k_2)\}} + \frac{-k_1[X^-]-k_{-2}\beta_2}{(\tau_1j\omega+2)\{k_1[X^-]+\beta_1(k_{-1}+4k_2)\}} \frac{\Delta\theta_2}{\Delta E} \quad (13)$$

$$\frac{\Delta\theta_2}{\Delta E} = \frac{ck_2\beta_1\theta_{1s}-\beta_2\theta_{2s}(-dk_{-2}+ek_3)-fk_{-3}[Pb(OH)_2]}{\beta_2(\tau_2j\omega+1)(k_{-2}+k_3)} + \frac{k_2\beta_1}{4\beta_2(\tau_2j\omega+1)(k_{-2}+k_3)} \frac{\Delta\theta_1}{\Delta E} \quad (14)$$

$$\tau_1 = \frac{\beta_1}{k_1[X^-] + \beta_1(k_{-1} + 4k_2)} \quad \tau_2 = \frac{1}{k_{-2} + k_3} \quad \text{where and}$$

Subsequently, from a current balance, the faradaic current flowing through the interface (at a steady state) is the sum of currents from each reaction, obtaining:

$$I_{Fs} = -F\{k_1(1 - \theta_{1s} - \theta_{2s})[X^-] - k_{-1}\beta_1\theta_{1s} + 16k_2\beta_1\theta_{1s} - 4k_{-2}\beta_2\theta_{2s} + 2k_3\beta_2\theta_{2s} - 2k_{-3}[Pb(OH)_2]\} \quad (15)$$

The application of  $\Delta E$  yields fluctuations of  $I_F$  as a function of  $E$  and  $\Delta\theta_n$  (n=1, 2):

$$\Delta I_F = \frac{\partial I_{Fs}}{\partial E} \Delta E + \frac{\partial I_{Fs}}{\partial \theta_1} \Delta\theta_1 + \frac{\partial I_{Fs}}{\partial \theta_2} \Delta\theta_2 \quad (16)$$

Evaluating the partial derivatives of equation (16) with equation (15), we obtain:

$$\Delta I_F = A\Delta E + F(k_1[X^-] + k_{-1}\beta_1 - 16k_2\beta_1)\Delta\theta_1 + F(k_1[X^-] + 4k_{-2}\beta_2 - 2k_3\beta_2) \Delta\theta_2 \quad (17)$$

Rearranging equation (17), the transfer function for faradaic impedance is obtained and given by:

$$\frac{1}{Z_F} = \frac{\Delta I_F}{\Delta E} = A + F(k_1[X^-] + k_{-1}\beta_1 - 16k_2\beta_1) \frac{\Delta\theta_1}{\Delta E} + F(k_1[X^-] + 4k_{-2}\beta_2 - 2k_3\beta_2) \frac{\Delta\theta_2}{\Delta E} \quad (18)$$

Here,

$$A = -F\{ak_1(1 - \theta_{1s} - \theta_{2s})[X^-] + bk_{-1}\beta_1\theta_{1s} + 16ck_2\beta_1\theta_{1s} + 4dk_{-2}\beta_2\theta_{2s} + 2ek_3\beta_2\theta_{2s} + 2fk_{-3}[Pb(OH)_2]\}$$

F is the faraday number, and  $a, b, c, d, e, f, k_{10}, k_{20}$  and  $k_{30}$  are fitting parameters, as described previously. Finally, the total impedance is calculated using the equivalent circuit shown in figure 1 to obtain expression (19):

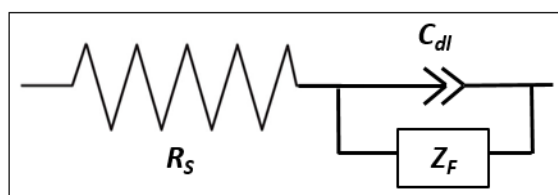


Figure 1. Equivalent circuit for total impedance.

$$Z_T = R_S + \frac{1}{C_{dl}(j\omega)^n + \frac{1}{Z_F}} \quad (19)$$

Resolving the system of equations (11)-(19), we can calculate  $Z_T$  for the proposed reaction mechanics.

### 3.2 Impedance spectrum fitting

As mentioned above, the fitting spectra are carried out from experimental spectra and equation (19) using the DE algorithm. The spectra shown in this work are the ones that showed the best fit (Table 1). Note that the function to minimize, equation (4), is not normalized with respect to the module,  $|Z|$ , so the fitness values are relatively high. On the other hand, it is important to point out that the data were normalized by subtracting the solution resistance,  $R_s$ , from the real parts of the impedance spectra.

Figure 2 shows the spectrum fitting for potentials of -0.5 and -0.4 V vs. SCE; at these potentials, only the capacitive effect [23] is observed because at these potentials, reactions (1), (2) and (3) are not favored, as previously explained.

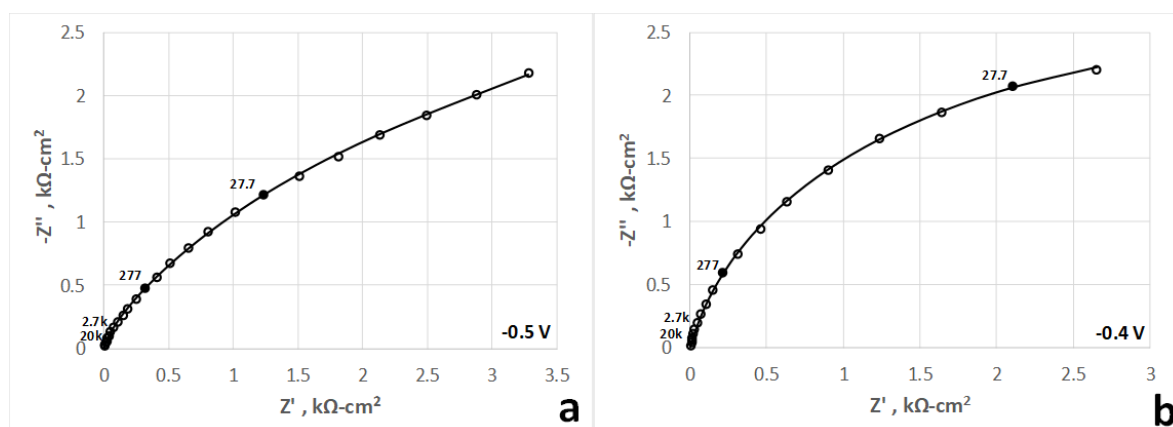


**Figure 2.** Complex impedance spectra for galena immersed in KCl solution at polarization potentials of a) -0.5 V and b) -0.4 V. The continuous lines are the fitted spectra by the DE algorithm. The frequency is in Hertz.

When the potential reaches the potential of zero charge (PZC) [14], at -0.3 V vs. SCE, (figure 3a), the presence of two time constants ( $\tau$ ) is evident. The first  $\tau$  is associated with reaction (1), which is included at  $Z_T$ , and coupled with a nonideal double-layer capacitance; as expected,  $k_I$  increases considerably (Table 1) with respect to the obtained values at -0.5 and -0.4 V vs. SCE. At frequencies below 1 Hz, a second  $\tau$  appears, which is associated with a pseudocapacitive effect due to the intermediate adsorption,  $X_{ads}$ , which blocks the electrode surface. The above can be evidenced by the  $\theta_I$  value, which shows that the  $X_{ads}$  covers the surface of the electrode in its entirety. This effect could explain the constant behavior of  $k_I$  even when the potential is increased to 0 and 0.1 V vs. SCE. This assumption agrees with the results found by other authors [12-13]. In figure 3b, the potential is

maintained at 0 V vs. SCE. In this case, the main differences observed in comparison with those of the spectrum at -0.3 SCE are the following: i) the loop is more depressed, and ii) the  $Z'$  value at 1 Hz is almost three times larger. The depressed loop can be explained by the overlapping of two time constants associated with reactions (1) and (2). According to the fitting, the increment of  $k_2$  by increasing the potential shows that reaction (2) is favored. However, we can again observe that the value of  $k_2$  remains almost constant at potentials of -0.3 V, 0 V and 0.1 V vs. SCE. This behavior can be explained by the blocking nature of the adsorbed intermediates  $X_{ads}$  and  $Pb(X)_{2ads}$  [15]. The reduction of  $C_{dl}$  when the potential is increased (Table 1) indicates that a more stable and compact layer of adsorbed intermediates are present at the electrode surface. Additionally, a third time constant associated with the incipient transfer charge process, reaction (3), is also observed at the limit of lowest frequencies and is noted in figure 3b.

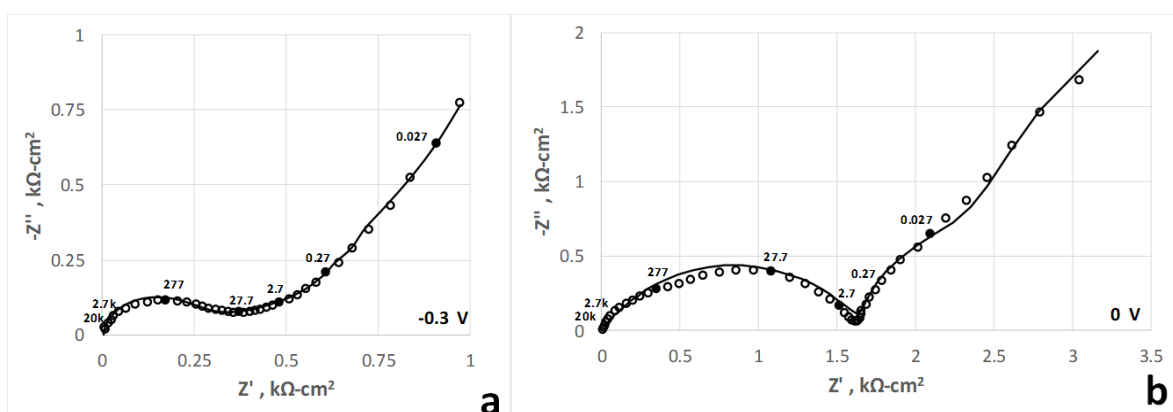


**Figure 3.** Complex impedance spectra for galena immersed in KCl solution at polarization potentials of a) -0.3 V and b) 0 V vs. SCE. The continuous lines are the fitted spectra of the DE algorithm. The frequency is in Hertz.

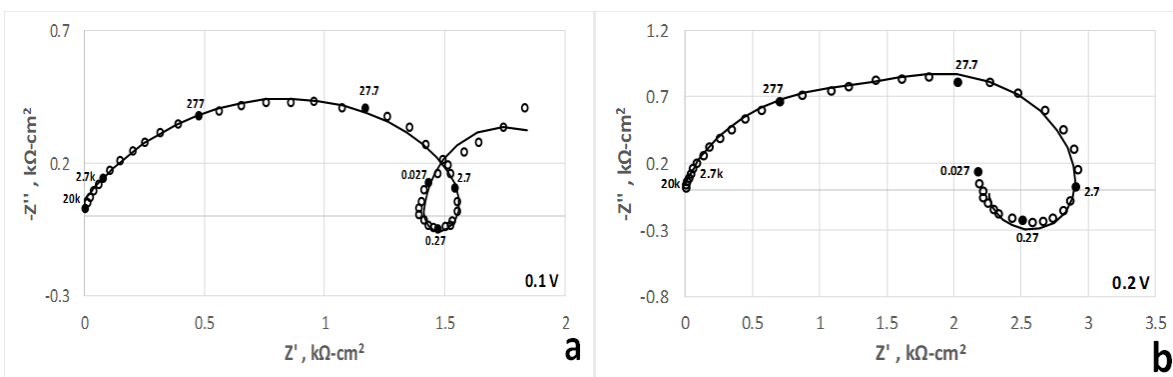


**Figure 4.** Complex impedance spectra for galena immersed in KCl solution at polarization potentials of a) 0.1 V and b) 0.2 V. The continuous lines are the fitted spectra of the DE algorithm. The frequency is in Hertz.

**Table 1.** Kinetic parameters obtained from the fitting of experimental impedance data from the approach of reaction mechanisms for galena in the presence of xanthate.

E (V)	$\beta_1$ (mol cm <sup>-2</sup> )	$\beta_2$ (mol cm <sup>-2</sup> )	$k_1$ (cm s <sup>-1</sup> )	$k_{-1}$ (cm s <sup>-1</sup> )	$k_2$ (cm s <sup>-1</sup> )	$k_{-2}$ (cm s <sup>-1</sup> )	$k_3$ (cm s <sup>-1</sup> )	$k_{-3}$ (cm s <sup>-1</sup> )
-0.5	1.26E-08	0.76E-10	5.31E-16	0.20E-16	4.54E-16	8.23E-16	1.47E-16	3.90E-16
-0.4	4.61E-08	0.48E-10	5.66E-14	659E-16	255E-16	242E-16	464E-16	725E-16
-0.3	474E-08	34.7E-10	3.27E-06	8.36E-05	82.9E-05	10E-03	1.43E-03	7.55E-06
-0.1	577E-08	3.80E-10	682E-06	93.9E-05	5.26E-05	56E-03	1.55E-03	5.16E-06
0	5.35E-08	835E-10	6.14E-06	4.65E-05	71.9E-05	11E-03	3.71E-03	35.2E-03
0.1	9.58E-08	2020E-10	3.29E-06	0.95E-05	60.3E-05	7E-03	49.58E-03	4.05E-03
0.2	0.49E-08	0.36E-10	235.53	197.05	340.23	67.70	38.15	508.81
E (V)	$a$ (V <sup>-1</sup> )	$b$ (V <sup>-1</sup> )	$c$ (V <sup>-1</sup> )	$d$ (V <sup>-1</sup> )	$e$ (V <sup>-1</sup> )	$f$ (V <sup>-1</sup> )		
-0.5	-46.634	-7.954	-20.935	-60.803	-138.249	-93.568		
-0.4	-57.133	-58.198	-43.160	-65.373	-87.366	17.540		
-0.3	-15.063	3.269	9.441	-15.350	-144.909	-92.097		
-0.1	14.088	-2.463	2.635	-42.607	-452.689	-265.335		
0	0.688	-4103.941	5.154	-6.800	35.695	3.040		
0.1	47.853	9.714	-16.126	2.835	1.224	-145.078		
0.2	-83.704	-62.098	-64.261	7.057	-40.339	-217.703		
E (V)	$C_{ad}$ ( $\Omega\text{cm}^{-2}\text{s}^n$ )	$n$	Pb(OH) <sub>2</sub> mol cm <sup>-3</sup>	$\theta_{1s}$	$\theta_{2s}$	fitness		
-0.5	7.17E-05	0.521	9.45E-05	0.999	65.4E-05	275.97		
-0.4	1.02E-05	0.863	16.1E-05	1.00	0.274E-05	317.73		
-0.3	547E-05	0.050	13.7E-05	1.00	2.72E-05	391.97		
-0.1	21.4E-05	0.254	18.8E-05	1.00	1.23E-05	942.26		
0	1.92E-05	0.607	2.63E-09	0.909	7.83E-02	2196.98		
0.1	1.45E-05	0.588	10.9E-05	.999	98.8E-05	863.52		
0.2	0.25E-05	0.754	0.106497	1.00	10.9E-05	1482.21		

At the potentials of 0.1 V and 0.2 V vs. SCE (figures 4a and 4b), three  $\tau$  values are observed, the first two are observed until 2.7 Hz and have the same physical meaning as those observed at -0.3 V vs. SCE. as previously explained. The third  $\tau$  can be observed as a well-defined inductive loop (figure 4b) associated with reaction (3). In accordance with figure 4 and Table 1, it is possible to observe that  $k_3$  and  $k_{-3}$  values have significantly changed. The inductive loops observed in figure 4 are associated with an interface relaxation process due to interfacial rearrangement that is caused by the adsorption-desorption of the adsorbed intermediates  $X_{ads}$  and  $Pb(X)_{2ads}$ . The explanation described above adequately matches other interpretations given for inductive loops by other authors [24-26]. According to Table 1, the values obtained for  $k_1$  and  $k_{-1}$  over the whole polarization potential range studied suggest that reaction (1) is the slowest; therefore, the adsorption of xanthate on the surface of galena is the predominant reaction. The above conclusion is evidenced from the values of  $\theta_{1s}$  and  $\theta_{2s}$ , which show that the surface of the electrode is covered mainly by  $X_{ads}$  adsorbate and could allow the preferential flotation of galena in flotation cells.

Finally, we can say that for all the polarization potentials, the values obtained for the cover fractions,  $\theta_{1s}$  and  $\theta_{2s}$ , vary between 0 and 1; therefore, the adjustments made are coherent and have physical sense.

Based on the previous discussion, it is possible to conclude that the parameters obtained from the adjustment using the DE algorithm are satisfactory; therefore, the proposed reaction mechanism for the oxidation and adsorption of xanthate on galena is valid. In this sense, the kinetic parameters obtained allow a better understanding of the oxidation of galena in the presence of xanthate and its influence on the hydrophilic and hydrophobic properties of metal sulfides.

#### 4. CONCLUSIONS

The fitting of EIS spectra for the PbS/X system under the approach of reaction mechanisms using the DE algorithm was satisfactory; therefore, the proposed mechanism for the oxidation and adsorption of xanthate on galena is valid. From this fact, we strongly recommend the use of optimization algorithms, such as DE, for the fitting of impedance spectra of any electrochemical system, even those with a complex reaction mechanism such as the one presented in this work. Interpretation of experimental measurements under the mechanistic point of view allows a deeper understanding of the physical-chemical nature of the process, which is desirable. In this context, the kinetic information obtained in this study allows a better understanding of the interfacial processes that occur during the oxidation of galena in the presence of xanthates and their influence on the processes involved in the separation of minerals by flotation.

#### References

1. T. Holm, S. Sunde, F. Seland and D.A. Harrington, *Electrochim. Acta*, (2019) 134764.
2. D.S. Ramírez-Rico, E.R. Larios-Durán, *J. Electrochem. Soc.*, 164 (2017) H994.
3. M. Gao, M.S. Hazelbaker, R. Kong and M.E. Orazem, *Electrochim. Acta*, 275 (2018) 119.
4. M.P. Gomes, I. Costa, N. Pébère, J.L. Rossi, B. Tribollet and V. Vivier, *Electrochim. Acta*, 306 (2019) 61.
5. G. Parrour, M. Chatenet and J.P. Diard, *Electrochim. Acta*, 55 (2010) 9113.
6. E.R. Larios-Durán and R. Antaño-López, *J. Electroanal. Chem.*, 658 (2011) 10.
7. Z. Nedjar and D. Barkat, *JESTEC*, 10 (2015), 932.
8. Y.L. Mikhlin, A.A. Karacharov and M.N. Likhatski, *Int. J. Miner. Process.*, 144 (2015) 81.
9. J.H. Chen, Y.Q. Li, L.H. Lan and J. Guo, *J. Ind. Eng. Chem.*, 20 (2014) 268.
10. B. McFadzean and C.T. O'Connor, *Miner. Eng.*, 65 (2014) 54.
11. L.H. Lan, J.H. Chen, Y.Q. Li, L.A.N. Ping, Y.A.N.G. Zhuo and G.Y. Ai, *Trans. Nonferrous Met. Soc. China*, 26 (2016) 272.
12. R. Woods, *J. Phys. Chem.*, 75 (1971) 354.
13. I.V. Chernyshova, *Langmuir*, 18 (2002) 6962.
14. E.D. Moreno-Medrano, N. Casillas, R. Cruz, R.H. Lara-Castro, M. Bárcena-Soto and E.R. Larios-Durán, *Int. J. Electrochem. Sci.*, 6 (2011) 6319.
15. D. Schuhmann, A.M. Guinard-Bacticle, P. Vanel and A. Talib, *J. Electrochem. Soc.*, 134 (1987) 1128.

16. A.R. Da Cruz, E.F. Wanner, R.T.N Cardoso and R.H.C. Takahashi, Using convex quadratic approximation as a local search operator in evolutionary multiobjective algorithms, In *Evolutionary Computation (CEC)*, 2011, IEEE Congress on, 1217.
17. S. Das, S.S. Mullick and P.N. Suganthan, *Swarm Evol. Comput.*, 27 (2016) 1.
18. S. Zhou, M. Liu, H. Chen and X. Li, *Int. J. Prod. Econ.*, 179 (2016) 1.
19. H.M. Hasanien, *Electr. Pow. Syst. Res.*, 157 (2018) 168.
20. M. Pirdashti, K. Movagharnejad, S. Curteanu, E.N. Dragoi and F. Rahimpour, *J. Ind. Eng. Chem.*, 27 (2015) 268.
21. R. Storn and K. Price, *J. Global Optim.*, 11 (1997) 341.
22. E. Barsoukov and J.R. Macdonald, *Impedance Spectroscopy Theory, Experiment and Applications*, 2nd ed. Wiley, (2005) New York, USA.
23. M.E. Orazem and B. Tribollet, *Electrochemical impedance spectroscopy*. Vol. 48 John Wiley & Sons, (2011) USA.
24. J. Chen, L. Lan and Y. Chen, *Miner. Eng.*, 46 (2013) 136.
25. I. Epolboin, M. Keddou and H. Takenouti, *J. Appl. Electrochem.*, 2 (1972) 71.
26. D.D. Macdonald, *J. Electrochem. Soc.*, 125 (1978) 2062.

© 2020 The Authors. Published by ESG ([www.electrochemsci.org](http://www.electrochemsci.org)). This article is an open access article distributed under the terms and conditions of the Creative Commons Attribution license (<http://creativecommons.org/licenses/by/4.0/>).